Radio Frequency Charge Parity Meter

M. D. Schroer,[1,*] M. Jung,[1] K. D. Petersson,[1] and J. R. Petta[1,2]
[1]Department of Physics, Princeton University, Princeton, New Jersey 08544, USA
[2]Princeton Institute for the Science and Technology of Materials (PRISM), Princeton University, Princeton, New Jersey 08544, USA
(Received 20 July 2012; published 17 October 2012)

$$f_c = \omega_c/2\pi \approx 560.9 \text{ MHz}$$

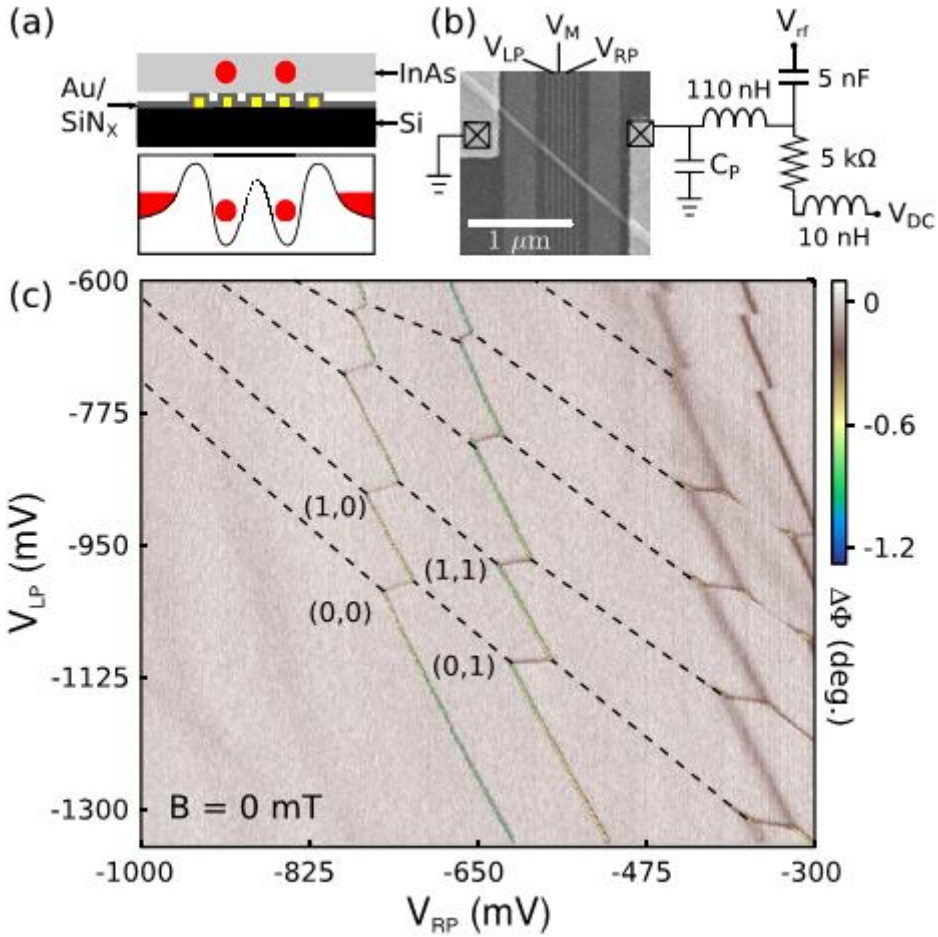

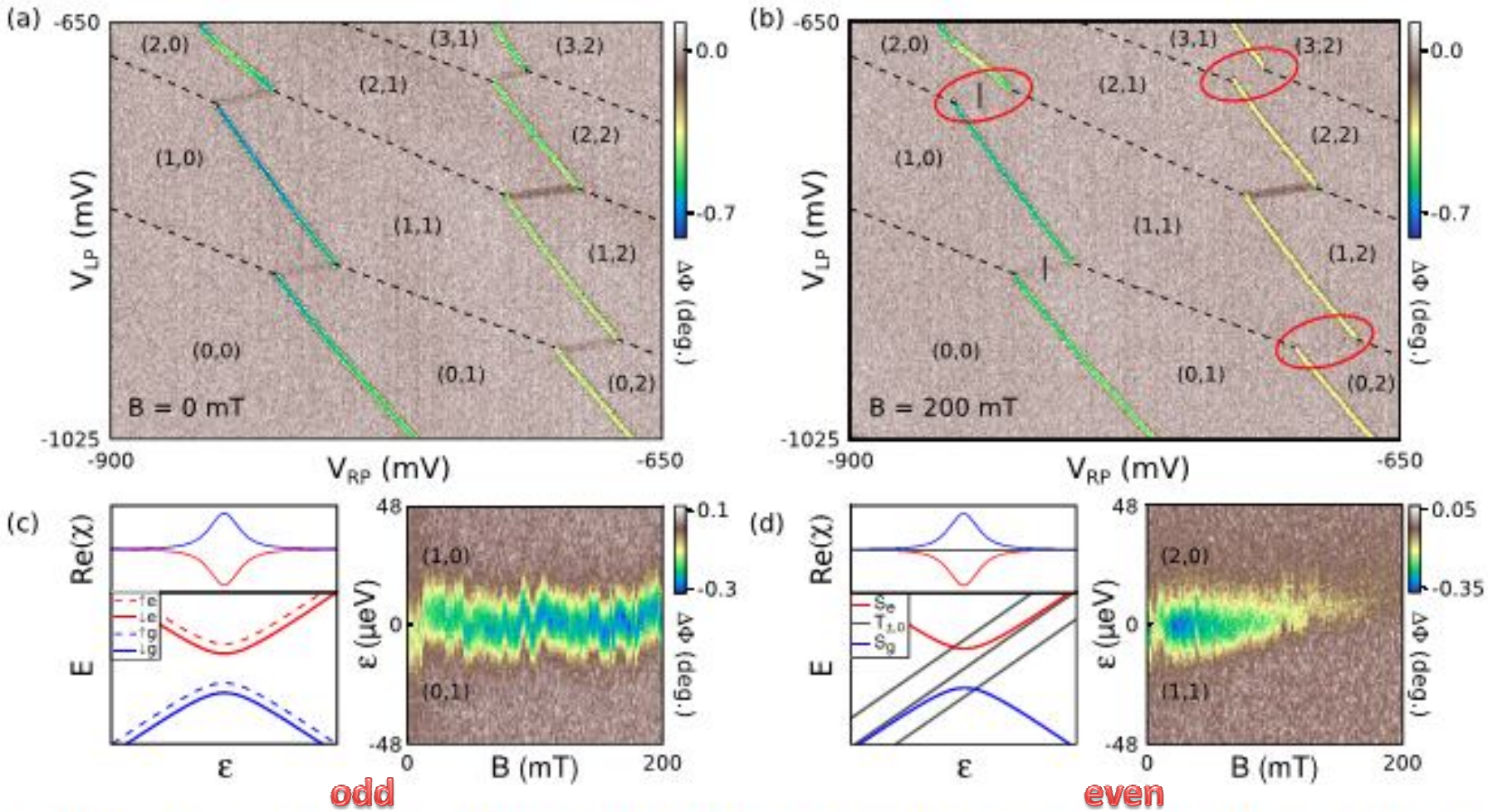

FIG. 2 (color online). The mesoscopic admittance of the DQD is sensitive to the total charge parity. (a) For $B = 0$ mT, a phase response is detected at all interdot transitions. (b) At $B = 200$ mT, the resonator is insensitive to charge dynamics at even parity charge transitions (circled in red). (c) Energy level diagram near the $(1, 0) \leftrightarrow (0, 1)$ charge transition. Charge dynamics in the double dot lead to an effective ac susceptibility, χ, which is maximal at $\epsilon = 0$. The ac susceptibility is largely insensitive to a magnetic field. (d) Energy level diagram near an even parity charge transition, e.g., $(2, 0) \leftrightarrow (1, 1)$. Pauli exclusion prohibits triplet tunneling near $\epsilon = 0$; however, singlet state tunneling is allowed. At large magnetic fields, the T_+ triplet state becomes the ground state and the ac susceptibility is greatly reduced, quenching the phase response of the resonator.

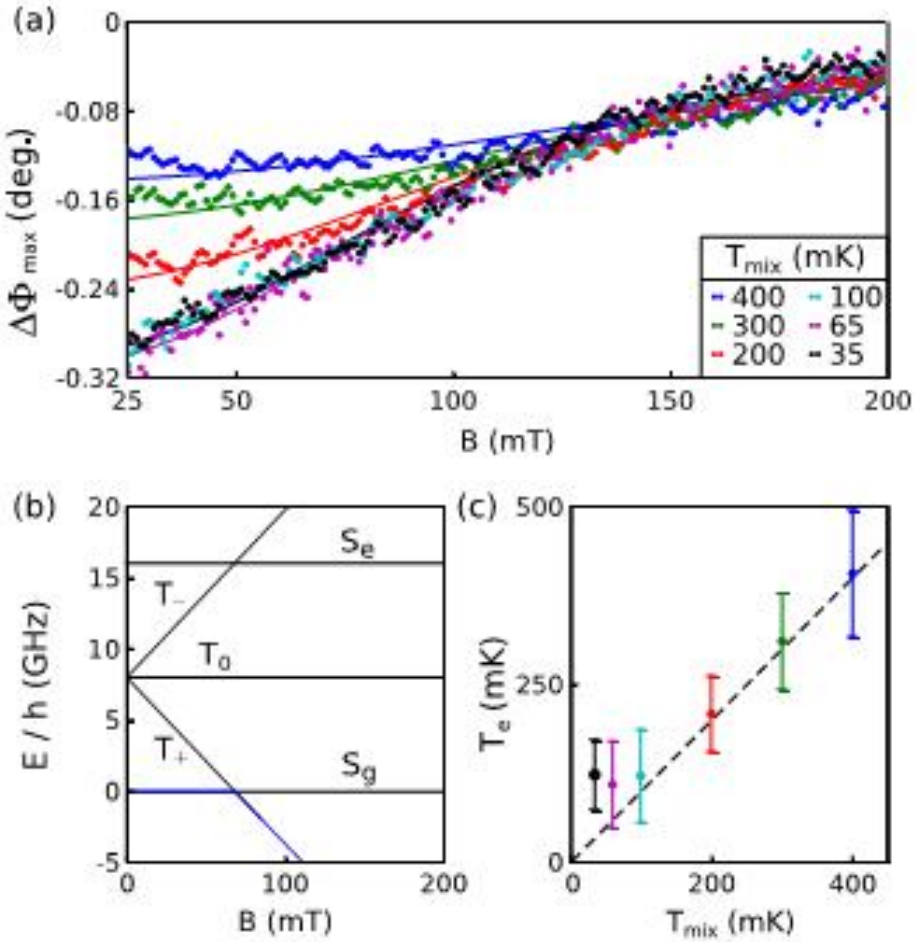

FIG. 3 (color online). Maximum phase shift, $\Delta\Phi_{max}$, plotted as a function of magnetic field for various temperatures. (a) Phase shifts extracted from data similar to Fig. 2(d), for temperatures from 35 to 400 mK. Fits to Eq. (3) are overlaid. (b) Relevant energy levels plotted as a function of magnetic field; the ground state is outlined in dark gray (blue). A thermally broadened suppression of the phase shift occurs as T_+ becomes the system's ground state. (c) Electron temperature, T_e, extracted from the fits to the data in (a) as a function of the mixing chamber temperature, T_{mix}. The electron temperature saturates at ~130 mK.

$$R = 1 + \frac{i\kappa}{\Delta_c/\hbar - i(\kappa + \kappa_i)/2 + g_{\text{eff}}\chi}$$

$$\langle\chi\rangle = \chi\left[\frac{e^{\Omega/2k_B T_e} - e^{-\Omega/2k_B T_e}}{Z(B, T_e)}\right],$$

$$R(B, T_e) = 1 + \frac{i\kappa}{\Delta_c/\hbar - i(\kappa + \kappa_i)/2 + g_{\text{eff}}\langle\chi\rangle}$$

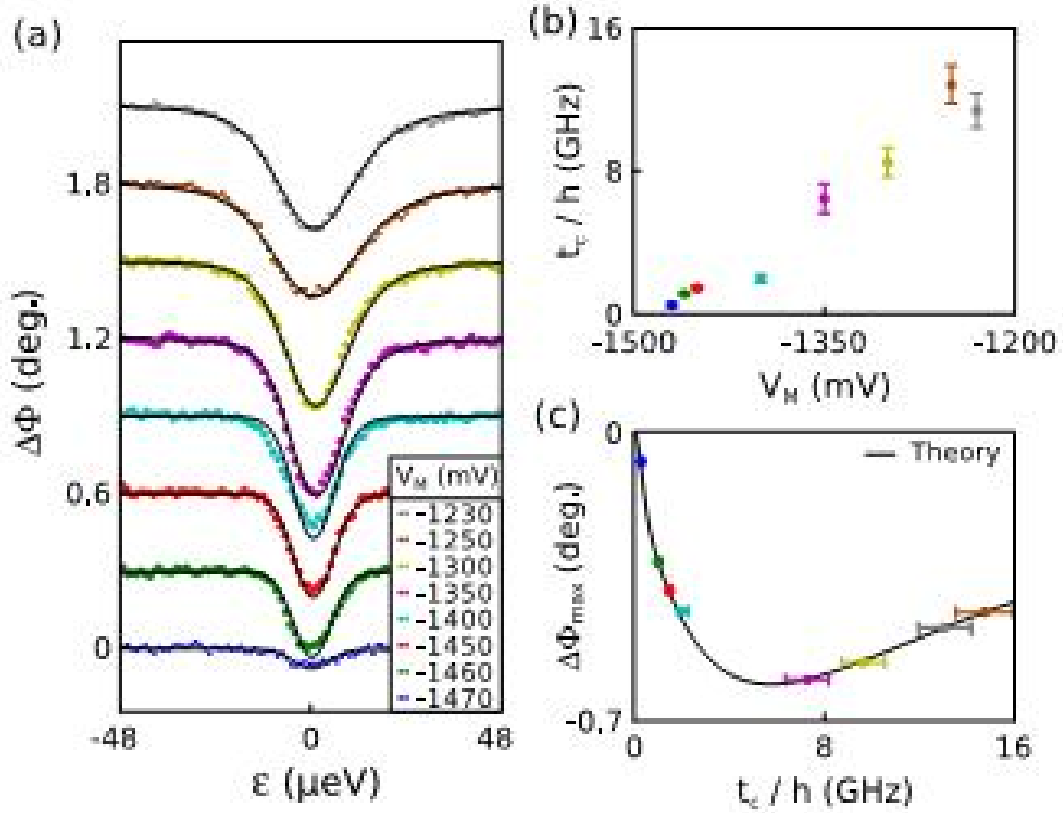

FIG. 4 (color online). Phase response as a function of interdot tunnel coupling. (a) Phase response at the $(2, 0) \leftrightarrow (1, 1)$ charge transition for middle gate voltages ranging from -1230 to -1470 mV. Each trace has been vertically offset by 0.3° for clarity. (b) The tunnel coupling extracted from the plots in (a). No signal is observable below a middle gate voltage of -1470 mV. (c) The maximum phase shift measured for each curve in (a) as a function of the extracted tunnel coupling. The solid line shows the theoretical response due to thermal mixing of the states at 130 mK; there is a strong suppression of the signal as the tunnel coupling approaches the thermal energy scale.